

Discovery of 4-(5-(4-Chlorophenyl)-2-methyl-3-propionyl-1H-pyrrol-1-yl)benzenesulfonamide (A-867744) as a Novel Positive Allosteric Modulator of the $\alpha 7$ Nicotinic Acetylcholine Receptor

Ramin Faghih,* Sujatha M. Gopalakrishnan, Jens Halvard Gronlien, John Malysz, Clark A. Briggs, Caroline Wetterstrand, Hilde Ween, Michael P. Curtis, Kathy A. Sarris, Gregory A. Gfesser, Rachid El-Kouhen, Holly M. Robb, Richard J. Radek, Kennan C. Marsh, William H. Bunnelle, and Murali Gopalakrishnan

Neuroscience Research, Global Pharmaceutical Research and Development, Abbott Laboratories, Abbott Park, Illinois 60064

Received January 19, 2009

The discovery of a series of pyrrole-sulfonamides as positive allosteric modulators (PAM) of $\alpha 7$ nAChRs is described. Optimization of this series led to the identification of **19** (A-867744), a novel type II PAM with good potency and selectivity. Compound **19** showed acceptable pharmacokinetic profile across species and brain levels sufficient to modulate $\alpha 7$ nAChRs. In a rodent model of sensory gating, **19** normalized gating deficits. These results suggest that **19** represents a novel class of molecules capable of allosteric modulation of the $\alpha 7$ nAChRs.

Introduction

$\alpha 7$ nAChRs^a play an important role in cognitive and sensory gating processes.^{1–3} The $\alpha 7$ subtype is distinguished from other nAChRs by its relatively high permeability to Ca^{2+} , rapid desensitization, and sensitivity to antagonists such as α -bungarotoxin and MLA.^{4–6} Current evidence, including validation by subtype selective agonists and antisense and gene knockout studies, supports the hypothesis that targeting the $\alpha 7$ nAChRs offers a symptomatic approach for treating a variety of cognitive and neurodegenerative disorders by modulating the release of neurotransmitters and activating phosphorylation events important for cognitive/attentive processes.^{7–10}

In recent years, a variety of structurally distinct subtype-selective $\alpha 7$ nAChR agonists have demonstrated efficacy in preclinical models of attention and cognitive deficits relevant to Alzheimer's disease and schizophrenia.^{11–17} An alternative approach is to enhance effects of the endogenous neurotransmitter acetylcholine (ACh) at $\alpha 7$ nAChRs via positive allosteric modulation, which could reinforce the endogenous cholinergic neurotransmission without directly activating $\alpha 7$ nAChRs.^{18,19} Indeed, such a positive allosteric modulator (PAM) approach has proven clinically successful for benzodiazepine modulation of GABA_A receptors.²⁰ Allosteric modulators bind at sites distinct, but as yet, undefined from the agonist-binding pocket^{21–23} and offer potential for better subtype selectivity than what has been achieved with agonists, thus exquisite subtype selectivity may be easier to achieve because the binding site(s) for PAMs are less highly conserved than the orthosteric site. Further, in principle, a PAM alone will not activate the receptor but will only amplify the physiological neurotransmitter signal in a

spatially and temporally restricted manner,²⁴ thus potentially offering differential efficacy and adverse effect profiles compared to agonists.

Initially disclosed nAChR PAMs, including bovine serum albumin,²⁵ acetylcholinesterase derived peptide SLURP-1,²⁶ and small molecules such as genistein,²⁷ galantamine,²⁸ and 5-hydroxyindole,²⁹ are generally weak and nonselective among nAChRs. More recently, a chemically heterogeneous group of molecules capable of differentially modulating nAChR properties have emerged (Figure 1). On the basis of the Monod–Wyman–Changeux model of allosteric interactions, at least two types of PAMs have been recognized: type I, which predominantly affects the peak current responses,^{30,31} and type II, which increases the peak current responses and changes the desensitization profile of the agonist response.^{32–35} Both types of PAMs have been reported to show in vivo efficacy in animal models of cognition and gating deficit.^{19,31,32} However, in some cases, in vitro properties and physiochemical properties remains to be further optimized, as compounds are limited by relatively low potency, low solubility, metabolic stability, and/or adequate CNS penetration. Accordingly, identification of selective, potent, and pharmacokinetically acceptable PAMs continues to be an active area of discovery research.

We reasoned that inclusion of PAMs, in particular those that affect receptor desensitization (Type II), should elicit $\alpha 7$ nAChR mediated Ca^{2+} flux, enabling detection by conventional high-throughput screening (HTS) approaches. Thus, after screening of the Abbott in-house compound library, the pyrrole-sulfonamides **10a** and **10b** (Figure 2) were identified as positive allosteric modulators of the $\alpha 7$ nAChR. However, initial hits were found to have low metabolic stability in a liver microsomes preparation and poor pharmacokinetic and CNS penetration properties in vivo (Table 1 and Figure 4). We considered that these shortcomings may result from metabolic liability contributed by the ester moiety. Preliminary studies on this template demonstrated that the presence of a *para*-phenylsulfonamide moiety on the pyrrole was essential for PAM activity at the $\alpha 7$ nAChR. We present below the synthesis and biological profile of a novel series of pyrrole-sulfonamides with improved microsomal stability and pharmacokinetics.

Chemistry. An initial objective of medicinal chemistry approaches was to identify lead compounds with superior

* To whom correspondence should be addressed. Phone: 847-9372972. Fax: 847-9374143. E-mail: ramin.faghih@abbott.com.

^a Abbreviations: nAChR, nicotinic acetylcholine receptor; SAR, structure–activity relationship; MLA, methyllycaconitine; ACh, acetylcholine; PAM, positive allosteric modulator; HTS, high-throughput screening; DMF, dimethylformamide; TEA, triethylamine; THF, tetrahydrofuran; DMA, dimethylacetamide; PS-DCC, polymer-supported 1,3-dicyclohexylcarbodiimide; HOBT, 1-hydroxybenzotriazole; CNS, central nervous system; FLIPR, fluorometric imaging plate reader; LC-MS, liquid chromatography–mass spectrometry; ESI-MS, electrospray ionization–mass spectrometry; SPE-MS, solid phase extraction–mass spectrometry; NADPH, nicotinamide adenine dinucleotide phosphate; HBSS, Hanks balanced salt solution; NMDG, *N*-methyl-D-glucosamine; HEPES, *N*-2-hydroxyethylpiperazine-*N'*-2-ethanesulfonic acid; POETs, parallel oocyte electrophysiology test station; EEG, electroencephalography; PBS, phosphate buffered saline.

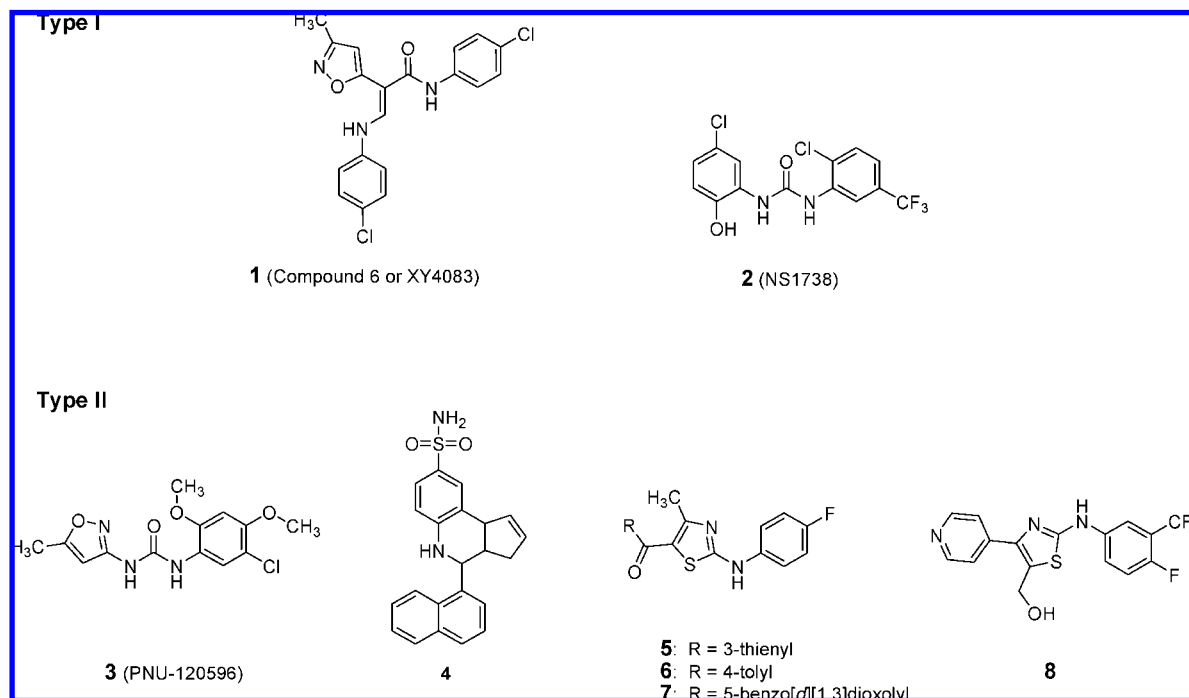


Figure 1. Examples of type I and type II allosteric modulators of $\alpha 7$ nAChR.

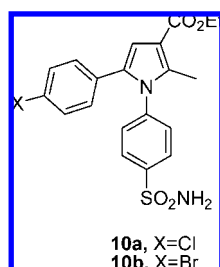


Figure 2. High-throughput screening hit.

metabolic stability while retaining in vitro modulation at the $\alpha 7$ nAChR. To accomplish this, the ethyl ester in **10a** was replaced with ketones (Scheme 1) and amides (Scheme 2) as functionalities that might lead to improved metabolic stability. A Paal–Knorr reaction³⁶ between the 1,4-butanedione **9** and 4-aminobenzenesulfonamide afforded compound **10a**.

Treatment of ester **10a** with sodium hydroxide in hot ethanol provided the carboxylic acid **11**. Compound **11** was transformed to its acid chloride with oxalyl chloride and DMF in THF followed by treatment with *N*-methyl-*O*-methyl hydroxylamine hydrochloride and triethylamine in CH_2Cl_2 to provide the Weinreb³⁷ amide **13** (Scheme 1). Compound **13** when treated with Grignard reagents provided the desired 3-keto-pyrrole-sulfonamides.

3-Amide-pyrrolesulfonamides were prepared by treating mixture of **11** and amines with PS-DCC³⁹ and HOBT in DMA/MeCN under microwave conditions (Scheme 2).

Results and Discussion

The SAR of a series of arylketones (Table 1) suggests that the addition of electron-withdrawing or donating groups to the aryl group does not improve in vitro potency as assessed by changes in $\alpha 7$ nAChR mediated intracellular Ca^{2+} fluorescence responses using FLIPR in human neuroblastoma (IMR-32) cells expressing native $\alpha 7$ nAChRs. The 4-methylphenyl and 4-chlorophenyl ketones (**14** and **17**) show at least 10-fold decrease in

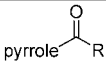
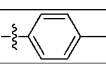
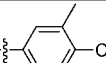
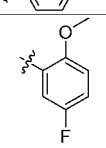
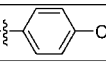
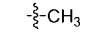
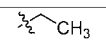
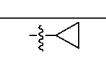
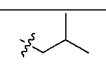
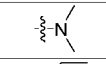
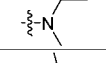
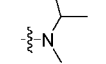
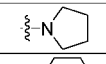
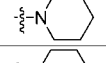
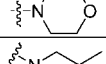
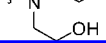
in vitro potency compared to **10a**, whereas the 4-chloro-3-methylphenyl ketone (**15**) shows a 2-fold decline in activity.

Aryl-ketones are inactive. On the other hand, alkyl-ketones exhibit modulator potencies equivalent or better than **10a** and offer improved efficacy as measured in the FLIPR assay. Moreover, for alkyl-ketone derivatives, steric factors seem to be important. Larger alkyl substituents on the carbonyl moiety slightly decrease PAM potency (e.g., **19** vs **20** and **21**). Overall, the amides were found to be much less potent than their alkyl-ketone counterparts except for the pyrrolidine amide **25** and analogues possessing moieties with additional binding properties (e.g., **28**). On the basis of its potency and excellent microsomal stability, compound **19** (A-867744) was selected for further characterization.

Compound **19** (0.1 nM to 10 μM) by itself did not evoke currents in *Xenopus* oocytes³⁹ expressing $\alpha 7$ nAChRs.⁴⁰ These data suggest that **19** does not directly activate $\alpha 7$ nAChRs. However, **19** enhanced acetylcholine-evoked currents in oocytes expressing $\alpha 7$ nAChRs. This potentiation was concentration-dependent, as demonstrated by measuring $\alpha 7$ currents evoked by ACh (100 μM) following brief preincubation with varying concentrations of **19** (Figure 3A). As depicted, **19** not only had a robust effect on the peak current response but also slowed the decay of the current response (Figure 3). Therefore, **19**, like urea **3**,³² (Figure 1) represents a novel type II positive allosteric modulator chemotype.

To further confirm the effect of **19** on $\alpha 7$ nAChR desensitization, responses to a selective $\alpha 7$ agonist, **29**,¹⁶ were measured in rat neonatal cortical neurons (Figure 3B). Compound **29** alone did not evoke Ca^{2+} fluorescence responses, which is attributable to rapid receptor desensitization within the time scale of detection. In the presence of 5 μM **19**, however, concentration-dependent increases in responses were observed, demonstrating that Ca^{2+} flux responses can be measured when $\alpha 7$ nAChR desensitization kinetics are altered by compound **19**. In contrast to effects at $\alpha 7$ nAChR, **19** (up to 30 μM) did not potentiate nicotine-evoked Ca^{2+} transients at human recombinant $\alpha 4\beta 2$ and $\alpha 3\beta 4$ nAChRs expressed in HEK-293 cell lines^{33,40} (data

Table 1. In vitro $\alpha 7$ nAChR PAM Activity and Microsomal Stability

Compound No.	pyrrole 	EC ₅₀ (μ M), Efficacy ^a	In vitro Metabolism (% remaining) ^b
10a	OEt	2.6 \pm 1.8 (22 \pm 5%)	3
10b	OEt	2.6 \pm 0.9 (20 \pm 4%)	2
11	OH	>30 (8 \pm 0.5%)	--
14		>30 (7 \pm 4%)	--
15		4.88 \pm 0.1 (9 \pm 1%)	38
16		10.5 \pm 1.3 (26 \pm 2%)	45
17		>30 (5 \pm 3%)	--
18		1.2 \pm 0.1 (39 \pm 5%)	64
19		1.0 \pm 0.6 (52 \pm 4%)	96
20		4.9 \pm 0.6 (25 \pm 4%)	92
21		3.9 \pm 0.4 (74 \pm 6%)	44
22		>30 (4 \pm 2%)	--
23		>30 (3%)	--
24		>30 (8 \pm 2%)	--
25		9.4 \pm 0.1 (57 \pm 1%)	31
26		>30 (11%)	--
27		>30 (5 \pm 1%)	--
28		3.6 \pm 0.1 (11 \pm 1%)	58

^a Compounds were tested in a cell-based fluorescent imaging plate reader (FLIPR) assay using human IMR-32 neuroblastoma that endogenously express $\alpha 7$ nAChRs.⁴¹ Application of test compound alone (up to 10 μ M) or $\alpha 7$ nAChR agonists such as **29** (PNU-282987) alone did not change intracellular Ca²⁺ levels. In contrast, when test compound was preapplied at concentrations ranging from 0.3 to 30 μ M, followed by subsequent addition of a fixed concentration of $\alpha 7$ agonist (10 μ M), concentration-dependent increases in fluorescence responses were detected. EC₅₀ values are means \pm standard deviation of 2–5 separate experiments, each conducted in duplicate, except, for example, **3** where $n = 9$. Numbers between parentheses indicated efficacy \pm standard deviation expressed as % of compound **3**.³² ^b In vitro metabolism in rat liver microsomes expressed as percent remaining at 30 min and are shown only for active compounds (efficacy >10%).

not shown). To further investigate its pharmacological specificity, **19** was tested for its ability to inhibit the binding of relevant ligands in a panel of receptor binding assays for >70 diverse neurotransmitter receptor and ion channel sites (CEREP, France). At the screening concentration of 10 μ M, no significant interaction at any of the targets (>50% displacement of test ligand) was observed. On the basis of its selectivity and potency, along with acceptable in vitro microsomal stability, compound **19** was selected for further characterization.

For agents targeted for treatment of CNS diseases, efficient brain penetration is of major importance. The high throughput screening hit **10a** had a very low brain:plasma ratio and achieved negligible brain concentrations (Figure 4A). In contrast, **19** achieved acceptable brain concentrations and favorable brain:plasma ratios.

Compound **19** was assessed for its PK properties in rat, dog, and monkey (Table 2). The animal pharmacokinetic profile of compound **19** was characterized by relatively low plasma clearance values (1.1–2.5 L/h/kg) and volumes of distribution (1.7–4.6 L/kg) across species, with terminal elimination half-lives in the 1.0–1.7 h. The bioavailability is 83% in rat and somewhat lower in dog (55%) and monkey (68%).

The $\alpha 7$ nAChR appears to play an important role in the filtering of afferent sensory input, a CNS function also referred to as gating.⁴³ For example, abnormal hippocampal $\alpha 7$ nAChR expression and function are linked to the inability of the DBA/2 mouse strain and schizophrenic patients to inhibit or “gate” evoked potential responding to repetitive auditory stimuli.^{8,43,44} Sensory gating deficits are thought to be related to the poor attention and cognitive function exhibited by schizophrenia patients. In a paired auditory stimulus paradigm, compound **19** (0.1–10.0 μ mol/kg, ip) improved sensory gating deficits when tested in vivo in the DBA/2 mouse. Like compounds **1**³⁰ and **3**,³³ compound **19** (Figure 5) significantly reduced the ratio of the response to test stimulus relative to the preceding response to conditioning stimulus ($T:C$ ratio). Reduced $T:C$ ratios are indicative of improved sensory gating, and the ability to lower $T:C$ ratios suggests that compound **19** may be useful to improve cognition in schizophrenia.

Brain concentrations of **19** after 0.1, 1.0, and 10.0 μ mol/kg, ip administrations were 2, 15, and 140 ng/g, respectively. Brain levels of **19** associated with minimally effective dose after 0.1 μ mol/kg ip administration is approximately 6 nM. This exposure overlaps with the lower range of the concentration–response determined from oocytes expressing rat $\alpha 7$ nAChRs (Figure 3A). These results suggest that a favorable response in vivo can be achieved at concentrations of PAM below that necessary to produce maximum effect in vitro.

Besides being efficacious in vivo, Compound **19** also possesses an excellent safety profile. It showed no inhibition of major liver metabolic enzymes such as CYP3A4, CYP2C9 (IC₅₀ > 10 μ M), and CYP2D6 (IC₅₀ = 2 μ M) and thus displays a low potential for drug–drug interactions. Compound **19** exhibited no significant hERG interactions (dofetilide binding K_i > 10 μ M, hERG IC₅₀ > 20 μ M). When tested in the anesthetized rat cardiovascular assays, compound **19** (3, 10, and 30 mg/kg achieving mean plasma concentrations of 1.0, 5.0, and 12.4 μ g/mL) did not display any significant effects on mean arterial pressure, heart rate, cardiac contractility (dP/dt @ 50 mmHg), or peripheral vascular resistance (data not shown).

Conclusions

In summary, optimization of the high-throughput screening hit **10a** led to the discovery of the pyrrole-sulfonamide **19**, a potent and selective $\alpha 7$ nAChR positive allosteric modulator. Compound **19** not only enhances the peak $\alpha 7$ nAChR current evoked by acetylcholine but also slows the desensitization profile of agonist responses. The excellent in vitro activity of this compound is matched by acceptable animal pharmacokinetics and safety profiles. Furthermore, **19** demonstrates efficacy to improve sensory gating in a rodent model, which suggests it may be useful in treating the cognitive deficits in schizophrenia. Thus, the pyrrole-sulfonamide **19** represents a novel chemotype

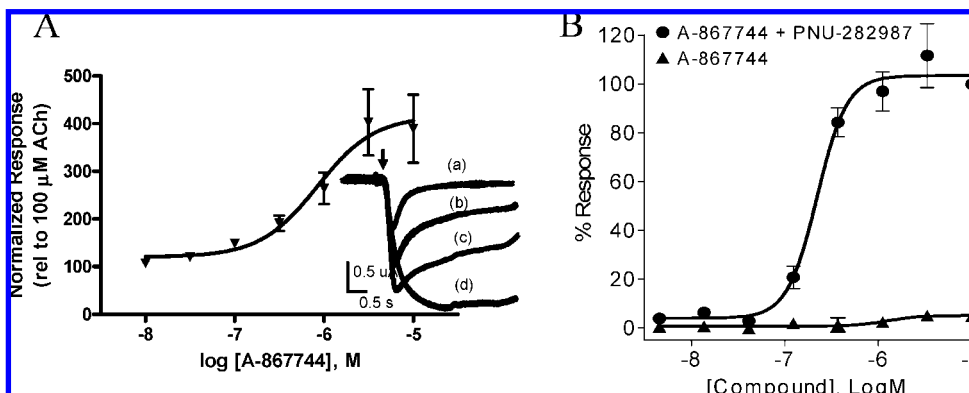
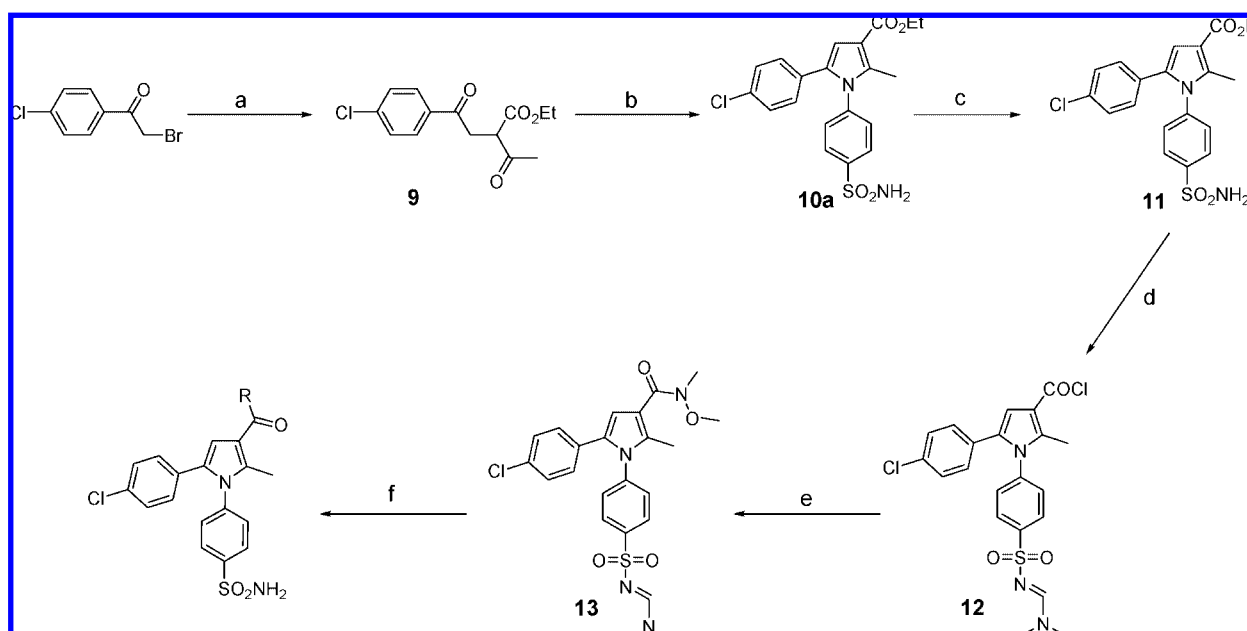


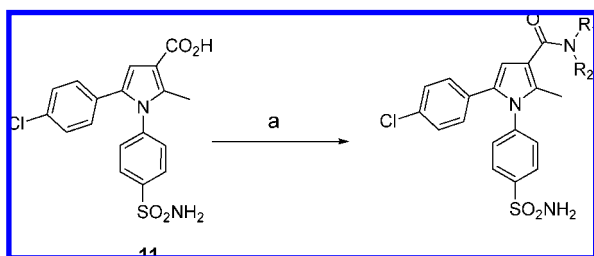
Figure 3. (A) Compound **19** enhances rat $\alpha 7$ nAChR-mediated currents in *Xenopus* oocytes. Inset: representative recording illustrating positive modulation of ACh-evoked currents by (a) no PAM, 0.3 (b), 1.0 (c), and 10 μ M (d) of **19** at $\alpha 7$ nAChRs. The arrow represents compound addition. (B) Increase in Ca^{2+} responses in IMR-32 cell line evoked by **19** (5 μ M) in presence of varying concentrations of the $\alpha 7$ nAChR agonist **29**.

Scheme 1. Synthesis of 3-Keto-pyrrolesulfonamide Derivatives^a



^a Reagents: (a) Ethylacetoacetate, K_2CO_3 , 2-butanone, reflux, 24 h; (b) 4-aminobenzenesulfonamide, glacial acetic acid, 100 $^\circ\text{C}$, 48 h; (c) NaOH (5 M), ethanol, reflux, 2 h; (d) oxalyl chloride, DMF, CH_2Cl_2 , 0 $^\circ\text{C}$ to room temperature, 3 h; (e) *N,O*-Dimethylhydroxylamine hydrochloride, TEA, CH_2Cl_2 , 0 $^\circ\text{C}$ to room temperature, 5 h; (f) RMgX , THF; aq HCl.

Scheme 2. Synthesis of 3-Amide-pyrrolesulfonamide Derivatives^a



^a Reagents: (a) PS-DCC, DMA, HOBT, Hunig's base, amines, MeCN, microwave, 100 $^\circ\text{C}$, 10 min.

useful in assessing whether a type II PAM displays advantages when compared to type I PAMs and ultimately to agonists in terms of efficacy, safety, and tolerability across preclinical models.

Experimental Section

All solvents were purchased from Aldrich (Sure/Seal anhydrous solvents), and commercially available reagents were used as received.

^1H NMR spectra were recorded on Varian Mercury (300 MHz) and Varian Unity (400 MHz). NMR data are reported in parts per million (δ) and are referenced to the tetramethylsilane as internal standard. Electron spray ionization (ESI) mass spectra were recorded on a Finnigan-400 instrument.

Analytical LC-MS was performed on a Finnigan Navigator mass spectrometer and Agilent 1100 HPLC system running Xcalibur 1.2, Open-Access 1.3, and custom login software. The mass spectrometer was operated under positive APCI ionization conditions. The HPLC system comprised an Agilent Quaternary pump, degasser, column compartment, autosampler, and diode-array detector, with a Sedere Sedex 75 evaporative light-scattering detector. The column used was a Phenomenex Luna Combi-HTS C8(2) 5 μm 100 \AA (2.1 mm \times 30 mm). A gradient of 10–100% acetonitrile (A) and 0.1% trifluoroacetic acid in water (B) was used at a flow rate of 2.0 mL/min (0–0.1 min 10% A, 0.1–2.6 min 10–100% A, 2.6–2.9 min 100% A, 2.9–3.0 min 100–10% A, 0.5 min post-run delay). Or a

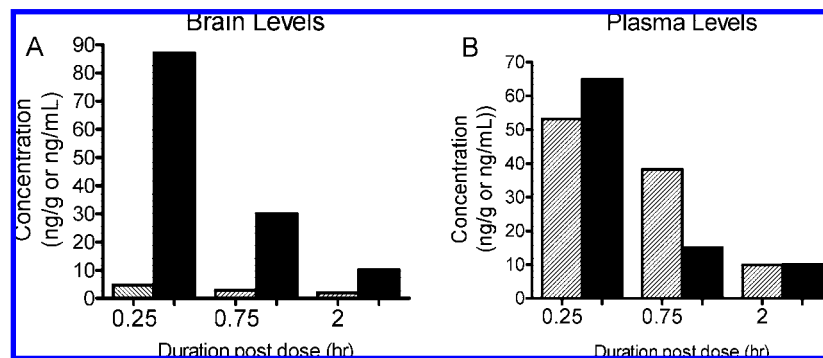


Figure 4. Brain and plasma concentrations of HTS hit **10a** (hatched bar) and **19** (solid bar) after administration of a 5 μ mol/kg ip dose in mouse.

Table 2. PK of Compound **19** in Rat, Dog, and Monkey^a

species	dose	$t_{1/2}$	V_{ss}	Cl_p	C_{max}	F
rat	2	1.7	4.6	2.1	41	83
dog	0.5/1	1.3	1.7	1.1	87	55
monkey	0.5/1	1.0	2.8	2.5	17	68

^a Units: dose iv and po (μ mol/kg), $t_{1/2}$ iv (h), V_{ss} iv (L/kg), Cl_p iv (L/h/kg), C_{max} po (ng/mL), F (%).

gradient of 10–100% acetonitrile (A) and 10 mM ammonium acetate in water (B) was used at a flow rate of 2.0 mL/min (0–0.1 min 10% A, 0.1–2.6 min 10–100% A, 2.6–2.9 min 100% A, 2.9–3.0 min 100–10% A, 0.5 min post-run delay) were used.

Chromatographic separations were performed on Analogix Super Flash columns or by preparative HPLC on a Phenomenex Luna C8(2) 5 μ m 100 Å AXIA column (30 mm \times 75 mm). A gradient of acetonitrile (A) and 0.1% trifluoroacetic acid in water (B) was used at a flow rate of 50 mL/min (0–0.5 min 10% A, 0.5–7.0 min linear gradient 10–95% A, 7.0–10.0 min 95% A, 10.0–12.0 min linear gradient 95–10% A). Samples were injected in 1.5 mL DMSO:MeOH (1:1). A custom purification system was used, consisting of the following modules: Waters LC4000 preparative pump, Waters 996 diode-array detector, Waters 717+ autosampler, Waters SAT/IN module, Alltech Vorex III evaporative light-scattering detector, Gilson 506C interface box, and two Gilson FC204 fraction collectors. The system was controlled using Waters Millennium32 software, automated using an Abbott developed Visual Basic application for fraction collector control and fraction tracking. Fractions were collected based upon UV signal threshold and selected fractions subsequently analyzed by flow injection analysis mass spectrometry using positive APCI ionization on a Finnigan LCQ using 70:30 MeOH:10 mM NH_4OH (aq) at a flow rate of 0.8 mL/min. Loop-injection mass spectra were acquired using a Finnigan LCQ running LCQ Navigator 1.2 software and a Gilson 215 liquid handler for fraction injection controlled by an Abbott developed Visual Basic application. Elemental combustion analyses were obtained from Robertson MicroLIT Laboratories. The purity of the compounds was analyzed by LC-MS, which showed $\geq 95\%$ purity for all compounds.

Ethyl 2-Acetyl-4-(4-chlorophenyl)-4-oxobutanoate (9). A mixture of 2-bromo-1-(4-chlorophenyl)ethanone (3.0 g, 12.8 mmol), ethyl acetoacetate (1.62 mL, 12.8 mmol), and potassium carbonate (4.5 g) was heated in 2-butanone (50 mL) at reflux for 24 h. Upon cooling, the mixture was filtered over celite and concentrated. The residue was purified by chromatography with CH_2Cl_2 to give the title compound in 78% yield. 1H NMR ($CDCl_3$): δ 1.31 (t, J = 8 Hz, 3H), 2.20 (s, 3H), 3.32 (m, 2H), 3.75 (m, 1H), 4.05 (m, 2H), 7.35 (d, J = 6.7 Hz, 2H), 7.83 (d, J = 6.7 Hz, 2H). MS (ESI) m/z 283 ($M + H$)⁺. Anal. ($C_{16}H_{15}BrClO_4$) C, H, N.

Ethyl 5-(4-Chlorophenyl)-2-methyl-1-(4-sulfamoylphenyl)-1H-pyrrole-3-carboxylate (10a). A mixture of ethyl 2-acetyl-4-(4-chlorophenyl)-4-oxobutanoate (3.3 g, 11.7 mmol) and sulfanilamide (2.01 g, 11.7 mmol) in glacial acetic acid (75 mL) was heated at 100 $^{\circ}C$ for 48 h. After cooling, the mixture was concentrated under reduced pressure. Ether (50 mL) was added to the residue

and the precipitate separated by filtration. The pale-yellow solid was washed with ether and dried. 1H NMR ($CDCl_3$): δ 1.31 (t, J = 8 Hz, 3H), 2.25 (s, 3H), 4.42 (m, 2H), 4.80 (m, 2H), 6.89 (s, 1H), 7.30–7.44 (m, 4H), 7.49–7.92 (m, 4H). MS (ESI) m/z 419 ($M + H$)⁺. Anal. ($C_{20}H_{19}ClN_2O_4S$) C, H, N.

5-(4-Chlorophenyl)-2-methyl-1-(4-sulfamoylphenyl)-1H-3-carboxylic Acid (11). The ethyl ester (4.19 g, 10 mmol) was suspended in ethanol (50 mL) and treated with 5 M NaOH (10 mL). The mixture was heated at reflux for 2 h. The suspension was filtered to collect a beige solid, which was rinsed with ethanol, stirred thoroughly in 1:1 EtOAc/ CH_2Cl_2 , recollected by filtration, and rinsed with more 1:1 EtOAc/ CH_2Cl_2 . The solid was dried under vacuum to give 2.18 g of the disodium salt as a light-beige powder. 1H NMR ($DMSO-d_6$): δ 2.32 (s, 3H), 6.54 (s, 1H), 6.98 (d, J = 8 Hz, 2H), 7.07 (d, J = 8 Hz, 2H), 7.20 (d, J = 8 Hz, 2H), 7.67 (d, J = 8 Hz, 2H). MS (ESI: negative ion detection) m/z 389/391. The disodium salt (0.94 g) was partitioned between EtOAc and 0.5 M aq HCl (10 mL) with stirring. Hexane was added, and the biphasic mixture was thoroughly stirred. The organic phase was separated, washed with water, dried (Na_2SO_4), and concentrated to give 744 mg of the free acid as a solid.

(E)-5-(4-Chlorophenyl)-1-(4-((dimethylamino)methylene)-sulfamoylphenyl)-2-methyl-1H-pyrrole-3-carboxyl Chloride (12). Oxalyl chloride (2 M in CH_2Cl_2 , 3.84 mL) was added dropwise at 0 $^{\circ}C$ to a solution of sodium carboxylate (1.5 g, 3.84 mmol) in CH_2Cl_2 (25 mL)/DMF (0.5 mL). Mixture was allowed to come to room temperature and stirred for 3 h. Mixture was concentrated under reduced pressure and used directly for the next step. MS (ESI) m/z 465 ($M + H$)⁺.

(E)-5-(4-Chlorophenyl)-1-(4-((dimethylamino)methylene)-sulfamoylphenyl)-N-methoxy-N-2-dimethyl-1H-Pyrrole-3-carboxamide (13). To a cold (0 $^{\circ}C$) mixture of pyrrole-acylchloride (1.9 g, 4.64 mmol) and *N,O*-dimethylhydroxylamine hydrochloride (0.5 g, 5.11 mmol) in CH_2Cl_2 (50 mL), TEA (1.62 mL, 11.6 mmol) was added. The reaction mixture was stirred at room temperature for 5 h. Solvent was evaporated and the residue purified by chromatography using a mixture of CH_2Cl_2 :MeOH (95:5). The desired compound was obtained in 70%. 1H NMR ($CDCl_3$): δ 2.25 (s, 3H), 3.05 (s, 3H), 3.20 (s, 3H), 3.42 (s, 3H), 3.80 (s, 3H), 6.75 (s, 1H), 6.91 (d, J = 8 Hz, 2H), 7.12 (d, J = 8 Hz, 2H), 7.23 (d, J = 8 Hz, 2H), 7.93 (d, J = 8 Hz, 2H), 8.17 (s, 1H). MS (ESI) m/z 489 ($M + H$)⁺. Anal. ($C_{23}H_{25}ClN_4O_4S \cdot H_2O$) C, H, N.

General Procedure for Grignard Coupling. To a solution of **13** (75 mg, 0.153 mmol) in anhydrous THF (5 mL) at room temperature, Grignard reagent (5 equiv) was added and the mixture heated to reflux and monitored by LC-MS. After cooling, the reaction was quenched by careful addition of a solution of saturated ammonium chloride (2 mL), water (5 mL), and extracted with CH_2Cl_2 . After drying the organic phase over sodium sulfate, solvent was removed under reduced pressure and the residue heated in a mixture of methanol (5 mL) and 5 N HCl (5 mL) and monitored by LC-MS. After cooling, the mixture was concentrated and the residue purified by reverse phase HPLC.

4-(5-(4-Chlorophenyl)-2-methyl-3-(4-methylbenzoyl)-1H-pyrrol-1-yl)benzenesulfonamide (14). ^1H NMR (CDCl_3): δ 2.26 (3H), 2.35 (3H), 6.75 (s, 1H), 7.10 (d, J = 8 Hz, 2H), 7.30 (d, J = 8 Hz, 2H), 7.35 (d, J = 8 Hz, 2H), 7.54 (m, 4H), 7.75 (d, J = 8 Hz, 2H), 7.92 (d, J = 8 Hz, 2H). MS (ESI) m/z 465 ($\text{M} + \text{H}$) $^+$. Anal. ($\text{C}_{25}\text{H}_{21}\text{ClN}_2\text{O}_3\text{S}$) C, H, N.

4-(3-(4-Chloro-3-methylbenzoyl)-5-(4-chlorophenyl)-2-methyl-1H-pyrrol-1-yl)benzenesulfonamide (15). ^1H NMR (CDCl_3): δ 2.32 (s, 3H), 2.43 (s, 3H), 6.66 (s, 1H), 7.09 (d, J = 8.5 Hz, 2H), 7.28 (d, J = 8.5 Hz, 2H), 7.59–7.78 (m, 5H), 7.91 (d, J = 8.5 Hz, 2H). MS (ESI) m/z 500 ($\text{M} + \text{H}$) $^+$. Anal. ($\text{C}_{25}\text{H}_{20}\text{Cl}_2\text{N}_2\text{O}_3\text{S} \cdot 0.5\text{H}_2\text{O}$) C, H, N.

4-(5-(4-Chlorophenyl)-3-(5-fluoro-2-methoxybenzoyl)-2-methyl-1H-pyrrol-1-yl)benzenesulfonamide (16). ^1H NMR (CDCl_3): δ 2.42 (s, 3H), 3.79 (s, 3H), 6.40 (s, 1H), 6.91 (d, J = 8.5 Hz, 2H), 6.94 (m, 1H), 7.11 (m, 6H), 7.30 (d, J = 8.5 Hz, 2H), 7.99 (d, J = 8.5 Hz, 2H). MS (ESI) m/z 499 ($\text{M} + \text{H}$) $^+$. Anal. ($\text{C}_{25}\text{H}_{20}\text{ClFN}_2\text{O}_4\text{S}$) C, H, N.

4-(3-(4-Chlorobenzoyl)-5-(4-chlorophenyl)-2-methyl-1H-pyrrol-1-yl)benzenesulfonamide (17). ^1H NMR (CDCl_3): δ 2.44 (s, 3H), 6.57 (s, 1H), 6.94 (d, J = 8.5 Hz, 2H), 7.17 (d, J = 8.5 Hz, 2H), 7.33 (d, J = 8.5 Hz, 2H), 7.47 (d, J = 8.5 Hz, 2H), 7.84 (d, J = 8.5 Hz, 2H), 8.01 (d, J = 8.5 Hz, 2H). MS (ESI) m/z 486 ($\text{M} + \text{H}$) $^+$. Anal. ($\text{C}_{24}\text{H}_{18}\text{Cl}_2\text{N}_2\text{O}_3\text{S}$) C, H, N.

4-(3-Acetyl-5-(4-chlorophenyl)-2-methyl-1H-pyrrol-1-yl)benzenesulfonamide (18). ^1H NMR ($\text{DMSO}-d_6$): δ 2.32 (s, 3H), 2.43 (s, 3H), 6.96 (s, 1H), 7.05 (d, J = 8.5 Hz, 2H), 7.30 (d, J = 8.5 Hz, 2H), 7.45 (d, J = 8.5 Hz, 2H), 7.88 (d, J = 8.5 Hz, 2H). MS (ESI) m/z 389 ($\text{M} + \text{H}$) $^+$. Anal. ($\text{C}_{19}\text{H}_{17}\text{ClN}_2\text{O}_3\text{S}$) C, H, N.

4-(5-(4-Chlorophenyl)-2-methyl-3-propionyl-1H-pyrrol-1-yl)benzenesulfonamide (19). ^1H NMR (CDCl_3): δ 1.24 (t, J = 7 Hz, 3H), 2.47 (s, 3H), 2.87 (q, J = 7.3 Hz, 2H), 6.74 (s, 1H), 7.17 (d, J = 8.5 Hz, 2H), 7.28 (d, J = 8.5 Hz, 2H), 7.98 (d, J = 8.5 Hz, 2H). MS (ESI) m/z 403 ($\text{M} + \text{H}$) $^+$. Anal. ($\text{C}_{20}\text{H}_{19}\text{ClN}_2\text{O}_3\text{S}$) C, H, N.

4-(5-(4-Chlorophenyl)-3-(cyclopropanecarbonyl)-2-methyl-1H-pyrrol-1-yl)benzenesulfonamide (20). ^1H NMR (CDCl_3): δ 0.96 (m, 2H), 1.21 (m, 2H), 2.47 (s, 3H), 2.49 (m, 1H), 6.90 (s, 1H), 6.95 (d, J = 8.5 Hz, 2H), 7.18 (d, J = 8.5 Hz, 2H), 7.28 (d, J = 8.5 Hz, 2H), 7.97 (d, J = 8.5 Hz, 2H). MS (ESI) m/z 415 ($\text{M} + \text{H}$) $^+$. Anal. ($\text{C}_{21}\text{H}_{19}\text{ClN}_2\text{O}_3\text{S} \cdot \text{H}_2\text{O}$) C, H, N.

4-(5-(4-Chlorophenyl)-2-methyl-3-(3-methylbutanoyl)-1H-pyrrol-1-yl)benzenesulfonamide (21). ^1H NMR (CDCl_3): δ 1.02 (d, J = 6 Hz, 6H), 2.31 (m, 1H), 2.44 (s, 3H), 2.69 (d, J = 6 Hz, 2H), 6.72 (s, 1H), 6.94 (d, J = 8.5 Hz, 2H), 7.17 (d, J = 8.5 Hz, 2H), 7.27 (d, J = 8.5 Hz, 2H), 7.98 (d, J = 8.5 Hz, 2H). MS (ESI) m/z 431 ($\text{M} + \text{H}$) $^+$. Anal. ($\text{C}_{22}\text{H}_{23}\text{ClN}_2\text{O}_3\text{S} \cdot 0.5\text{H}_2\text{O}$) C, H, N.

General Procedure for Amide Formation. In a microwave vial containing 3 equiv of PS-DCC, a solution of **11** (29 mg, 0.06 mmol) in DMA (1.0 mL) was added, followed in succession by a solution of 1-hydroxybenzotriazole (8 mg, 0.06 mmol) in acetonitrile (0.6 mL), and a solution of *N,N*-diisopropylethylamine (23 mg, 0.18 mmol) in acetonitrile (0.6 mL). Then a solution of the amine (0.07 mmol) in acetonitrile (0.4 mL) was added. The mixture was heated in the microwave (Emrys Optimizer/Biotage) to 100 °C for 600 s. The reaction was filtered through a Si-carbonate cartridge (Sili-Cycle) and concentrated to dryness. The residues were purified by preparative HPLC.

5-(4-Chlorophenyl)-*N,N*,2-trimethyl-1-(4-sulfamoylphenyl)-1H-pyrrole-3-carboxamide (22). ^1H NMR ($\text{DMSO}-d_6/\text{D}_2\text{O}$) δ 2.09 (s, 3H), 3.83 (s, 6H), 6.55 (s, 1H), 7.05 (d, J = 8.5 Hz, 2H), 7.27 (d, J = 8.5 Hz, 2H), 7.46 (d, J = 8.5 Hz, 2H), 7.88 (d, J = 8.5 Hz, 2H). MS (ESI: negative ion detection) m/z 416 ($\text{M} - \text{H}$) $^-$. Anal. ($\text{C}_{20}\text{H}_{20}\text{ClN}_3\text{O}_3\text{S}$) C, H, N.

5-(4-Chlorophenyl)-*N*-ethyl-*N*,2-dimethyl-1-(4-sulfamoylphenyl)-1H-pyrrole-3-carboxamide (23). ^1H NMR ($\text{DMSO}-d_6/\text{D}_2\text{O}$) δ 1.13 (t, J = 7 Hz, 3H), 2.09 (s, 3H), 3.38 (s, 3H), 3.46 (m, 2H), 6.51 (s, 1H), 7.05 (d, J = 8.5 Hz, 2H), 7.27 (d, J = 8.5 Hz, 2H),

7.46 (d, J = 8.5 Hz, 2H), 7.88 (d, J = 8.5 Hz, 2H). MS (ESI: negative ion detection) m/z 430 ($\text{M} - \text{H}$) $^-$. Anal. ($\text{C}_{21}\text{H}_{22}\text{ClN}_3\text{O}_3\text{S}$) C, H, N.

5-(4-Chlorophenyl)-*N*-isopropyl-*N*,2-dimethyl-1-(4-sulfamoylphenyl)-1H-pyrrole-3-carboxamide (24). ^1H NMR ($\text{DMSO}-d_6/\text{D}_2\text{O}$) δ 1.15 (d, J = 7 Hz, 6H), 2.08 (s, 3H), 3.38 (m, 4H), 6.48 (s, 1H), 7.05 (d, J = 8.5 Hz, 2H), 7.27 (d, J = 8.5 Hz, 2H), 7.46 (d, J = 8.5 Hz, 2H), 7.88 (d, J = 8.5 Hz, 2H). MS (ESI: negative ion detection) m/z 444 ($\text{M} - \text{H}$) $^-$. Anal. ($\text{C}_{22}\text{H}_{24}\text{ClN}_3\text{O}_3\text{S} \cdot \text{H}_2\text{O}$) C, H, N.

5-(4-Chlorophenyl)-2-methyl-3-(pyrrolidine-1-carbonyl)-1H-pyrrol-1-yl)benzenesulfonamide (25). ^1H NMR ($\text{DMSO}-d_6/\text{D}_2\text{O}$) δ 1.85 (m, 4H), 2.18 (s, 3H), 3.45 (m, 2H), 3.64 (m, 2H), 6.68 (s, 1H), 7.05 (d, J = 8.5 Hz, 2H), 7.27 (d, J = 8.5 Hz, 2H), 7.46 (d, J = 8.5 Hz, 2H), 7.88 (d, J = 8.5 Hz, 2H). MS (ESI: negative ion detection) m/z 442 ($\text{M} - \text{H}$) $^-$. Anal. ($\text{C}_{22}\text{H}_{22}\text{ClN}_3\text{O}_3\text{S}$) C, H, N.

5-(4-Chlorophenyl)-2-methyl-3-(piperidine-1-carbonyl)-1H-pyrrol-1-yl)benzenesulfonamide (26). ^1H NMR ($\text{DMSO}-d_6/\text{D}_2\text{O}$) δ 1.59 (m, 4H), 1.62 (m, 2H), 2.09 (s, 3H), 3.56 (m, 4H), 6.46 (s, 1H), 7.05 (d, J = 8.5 Hz, 2H), 7.27 (d, J = 8.5 Hz, 2H), 7.46 (d, J = 8.5 Hz, 2H), 7.88 (d, J = 8.5 Hz, 2H). MS (ESI: negative ion detection) m/z 456 ($\text{M} - \text{H}$) $^-$. Anal. ($\text{C}_{23}\text{H}_{22}\text{ClN}_3\text{O}_3\text{S} \cdot \text{H}_2\text{O}$) C, H, N.

5-(4-Chlorophenyl)-2-methyl-3-(morpholine-1-carbonyl)-1H-pyrrol-1-yl)benzenesulfonamide (27). ^1H NMR ($\text{DMSO}-d_6/\text{D}_2\text{O}$) δ 2.10 (s, 3H), 3.61 (m, 8H), 6.52 (s, 1H), 7.06 (d, J = 8.5 Hz, 2H), 7.27 (d, J = 8.5 Hz, 2H), 7.46 (d, J = 8.5 Hz, 2H), 7.90 (d, J = 8.5 Hz, 2H). MS (ESI: negative ion detection) m/z 458 ($\text{M} - \text{H}$) $^-$. Anal. ($\text{C}_{22}\text{H}_{22}\text{ClN}_3\text{O}_4\text{S}$) C, H, N.

5-(4-Chlorophenyl)-*N*-(2-hydroxyethyl)-2-methyl-*N*-propyl-1-(4-sulfamoylphenyl)-1H-pyrrole-3-carboxamide (28). ^1H NMR ($\text{DMSO}-d_6/\text{D}_2\text{O}$) δ 0.96 (t, J = 7 Hz, 3H), 1.60 (m, 2H), 2.09 (s, 3H), 3.41–3.46 (m, 2H), 3.46–3.52 (m, 2H), 3.53–3.64 (m, 2H), 6.50 (s, 1H), 6.97–7.10 (2H), 7.05 (d, J = 8.5 Hz, 2H), 7.27 (d, J = 8.5 Hz, 2H), 7.46 (d, J = 8.5 Hz, 2H), 7.88 (d, J = 8.5 Hz, 2H). MS (ESI: negative ion detection) m/z 474 ($\text{M} - \text{H}$) $^-$. Anal. ($\text{C}_{23}\text{H}_{26}\text{ClN}_3\text{O}_4\text{S}$) C, H, N.

In Vitro Metabolism. Microsomes were distributed to 96-well plates and warmed for 10 min at 37 °C in the on-deck incubator. Compound and NADPH were mixed in a 96 deep-well plate and the mixture delivered in triplicate to the warm microsomes to initiate the reaction. In the incubation mixture, the final reagent concentrations were as follows: NADPH 1 mM, compound 1 μM , and microsomal protein 0.5 mg/mL. After incubation for 0, 10, 20, and 30 min, reactions were stopped by protein precipitation with one volume of acetonitrile/methanol containing 0.4 μM warfarin, the internal standard. Samples were then centrifuged at 3400 rpm for 45 min, and the clarified supernatant was transferred to 96-well plates and divided for SPE-MS preparation and HPLC-MS analysis.

Fluorescence Measurements. Changes in intracellular Ca^{2+} levels were measured using calcium-4 no-wash dye as previously described.³² Briefly, IMR-32 cells were grown as a monolayer in black-walled clear-bottom plates coated with poly-D-lysine (BD Biosciences, Bedford, MA). Prior to the assay, culture media was discarded and cells loaded no-wash dye in NMDG buffer (10 mM HEPES, pH 7.4, 140 mM *N*-Methyl-D-glucosamine (NMDG), 5 mM KCl, 1 mM MgCl_2 , 10 mM CaCl_2 for 1 h at 25 °C). Primary rat neonatal cortical neurons were isolated from newborn rat pups (E18) and cultured,⁴⁴ except that cells were plated onto poly D-lysine-coated black-walled 384-well plates at a density of 10000 cells/well. Experiments were conducted 3 days postplating. Changes in cellular Ca^{2+} levels were measured as described above, except that assays were conducted using calcium-3 dye prepared in Hank's balanced salt solution buffer (HBSS) containing 20 mM HEPES as described by the manufacturer (MDS Analytical Technologies, Sunnyvale, CA). In both cases, after a baseline reading for 10 s, modulator/test compounds were added to the cell plate and incubated for 3–5 min. This was followed by the addition of appropriate concentrations of agonist. The peak increase in fluorescence over baseline was determined and is expressed as relative fluorescence units (RFU), normalized to the maximal value.

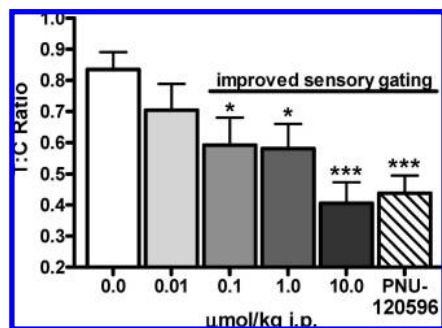


Figure 5. Compound **19** improved sensory gating in DBA/2 mice by significantly lowering $T:C$ ratios. One-way repeated measures ANOVA $F(5,59) = 6.393$, $p < 0.0001$. * $p < 0.05$, *** $p < 0.001$ vs vehicles, Newman–Keuls post hoc test. Compound **3** was dosed at $30.0 \mu\text{mol/kg}$ i.p. For experimental details, see ref 43.

Two-Electrode Voltage Clamp Studies. Oocytes were obtained from adult female *Xenopus laevis* frogs (Blades Biological Ltd., Cowden, Edenbridge, Kent, UK) and cared for in accordance with the Institutional Animal Care Committee guidelines that meet the guidelines of the National Institutes of Health. Chemicals and reagents were obtained from Sigma or Fisher Scientific (Essex, UK).

Xenopus laevis oocytes were prepared for electrophysiological experiments as described.³² Briefly, 3–4 lobes from ovaries of female adult *Xenopus laevis* frogs were removed, manually defolliculated, treated with collagenase type 1A (2 mg/mL, Sigma) prepared in low- Ca^{2+} Barth's solution (in mM: 90 NaCl, 1.0 KCl, 0.66 NaNO_3 , 2.4 NaHCO_3 , 10 HEPES, 2.5 Na-pyruvate, 0.82 MgCl_2 , and 0.5% v/v penicillin–streptomycin solution, pH = 7.55) for 1.5–2 h at $\sim 18^\circ\text{C}$ under constant agitation to obtain isolated oocytes. The oocytes were injected with ~ 20 – 25 ng nAChR cRNA, kept at 18°C in a humidified incubator in modified Barth's solution (in mM: 90 NaCl, 1.0 KCl, 0.66 NaNO_3 , 2.4 NaHCO_3 , 10 HEPES, 2.5 Na-pyruvate, 0.74 CaCl_2 , 0.82 MgCl_2 , 0.5% v/v penicillin–streptomycin solution, pH = 7.55), and used 2–7 days after injection. Responses were measured by two-electrode voltage clamp techniques using POETs. During recordings, the oocytes were bathed in Ba^{2+} -OR2 solution (in mM: 90 NaCl, 2.5 KCl, 2.5 BaCl_2 , 1.0 MgCl_2 , 5.0 HEPES, 0.0005 atropine, pH = 7.4) and held at -60 mV at room temperature. Agonists were applied to the recording chamber for 1 s at 6 mL/s with or without modulators. Test compounds were applied for a minimum of 60 s prior to agonist application. In two electrode voltage clamp studies, responses were quantified by measuring apparent peak current amplitude. Apparent peak current responses were expressed as percentage response to $100 \mu\text{M}$ ACh in modulator concentration responses. Data were analyzed and fitted using GraphPad Prism (San Diego, CA). Sigmoidal dose–response (variable slope) function was used to fit the replicates. The pEC_{50} ($-\log \text{EC}_{50}$) or pIC_{50} ($-\log \text{IC}_{50}$) values and associated standard error of the mean (SEM) were obtained from fitted results. The maximum mean \pm SEM values were calculated from individual experiments.

N40 Gating. DBA/2 mice (16–20 g, Harlan) were used for N40 gating experiments and surgical techniques employed were similar to those previously described.⁴³ Briefly, mice were anesthetized with a solution of 2.8% ketamine, 0.28% xylazine, 0.05% acepromazine, and stereotactically implanted with tripolar stainless steel wire electrodes for EEG recordings in the CA3 region of the hippocampus. Animals were allowed to recover for at least four days before conducting experiments. Auditory evoked potentials were generated by presentation of 120 sets of paired white noise bursts (5 ms duration) from a speaker within the recording chamber at a distance of approximately 15–20 cm from the mouse. The first auditory stimulus of the pair, or conditioning stimulus (C), was followed 0.5 s later by the second auditory stimulus (test stimulus, T). The length of time between stimulus pairs was 15 s. Data acquisition software (SciWorks, Datawave Technologies, Berthoud, CO) recorded EEG signals 100 ms before and for 900

ms after the initial conditioning stimulus. The software averaged the 120 paired responses into one composite evoked potential (EP) response. The amplitude of the auditory EP N40 wave was determined for both the averaged conditioning (C) and test (T) EP response, and a ratio ($T:C$ ratio) was derived between the two responses by dividing the test amplitude by the conditioning amplitude. The $T:C$ ratio was the index by which compound efficacy was determined. The vehicle for **19** and **3** was 5% DMSO and 5% Solutol in PBS. Compound was administered immediately before mice were placed into the recording chambers and initiation of auditory evoked potential recording. Recording of paired auditory evoked potentials continued for 30 min after the recordings began. For every experiment, each mouse was administered all treatments including a control vehicle in random order on separate days with at least 72 h between treatments. This within-subjects design allowed each mouse to serve as its own control. Data are expressed as means \pm SEM. Significant differences between group means were assessed by one-way analysis of variance (ANOVA), and Newman–Keuls post hoc tests assessed differences between treatment groups (GraphPad Software Inc., San Diego, CA). A p value < 0.05 was considered statistically significant.

Supporting Information Available: LC/MS analyses data for compounds **11** and **19** and hemodynamic evaluation of compound **19** in the rat cardiovascular model. This material is available free of charge via the Internet at <http://pubs.acs.org>.

References

- (1) Olincy, A.; Harris, J. G.; Johnson, L. L.; Pender, V.; Kongs, S.; Allensworth, D.; Ellis, J.; Zerbe, G. O.; Leonard, S.; Stevens, K. E.; Stevens, J. O.; Martin, L.; Adler, L. E.; Soti, F.; Kem, W. R.; Freedman, R. Proof-of-concept trial of an $\alpha 7$ nicotinic agonist in schizophrenia. *Arch. Gen. Psychiatry* **2006**, *63*, 630–638.
- (2) Young, J. W.; Crawford, N.; Kelly, J. S.; Kerr, L. E.; Marston, H. M.; Spratt, C.; Finlayson, K.; Sharkey, J. Impaired attention is central to the cognitive deficits observed in $\alpha 7$ deficient mice. *Eur. Neuropsychopharmacol.* **2007**, *17*, 145–155.
- (3) Adler, L. E.; Olincy, A.; Waldo, M.; Harris, J. G.; Griffith, J.; Stevens, K.; Flach, K.; Nagamoto, H.; Bickford, P.; Leonard, S.; Freedman, R. Schizophrenia, sensory gating and nicotinic receptors. *Schizophrenia Bull.* **1998**, *24*, 189–202.
- (4) Dajas-Bailador, F.; Wonnacott, S. Nicotinic acetylcholine receptors and the regulation of neuronal signalling. *Trends Pharmacol. Sci.* **2004**, *25*, 317–324.
- (5) Castro, N. G.; Albuquerque, E. X. α -Bungarotoxin-sensitive hippocampal nicotinic receptor channel has a high calcium permeability. *Biophys. J.* **1995**, *68*, 516–524.
- (6) Seguela, P.; Wadiche, J.; Dineley-Miller, K.; Dani, J. A.; Patrick, J. W. Molecular cloning, functional properties, and distribution of rat brain $\alpha 7$: a nicotinic cation channel highly permeable to calcium. *J. Neurosci.* **1993**, *13*, 596–604.
- (7) Mazurov, A.; Hauser, T.; Miller, C. H. Selective $\alpha 7$ nicotinic acetylcholine receptor ligands. *Curr. Med. Chem.* **2006**, *13*, 1567–1584.
- (8) Bitner, R. S.; Bunnelle, W. H.; Anderson, D. J.; Briggs, C. A.; Buccafusco, J.; Curzon, P.; Decker, M. W.; Frost, J. M.; Gronlien, J. H.; Gubbins, E.; Li, J.; Malysz, J.; Markosyan, S.; Marsh, K.; Meyer, M. D.; Nikkel, A. L.; Radek, R. J.; Robb, H. M.; Timmermann, D.; Sullivan, J. P.; Gopalakrishnan, M. Broad-spectrum efficacy across cognitive domains by $\alpha 7$ nicotinic acetylcholine receptor agonism correlates with activation of ERK1/2 and CREB phosphorylation pathways. *J. Neurosci.* **2007**, *27*, 10578–10587.
- (9) Bouvraï-Veret, C.; Weiss, S.; Andrieux, A.; Schweitzer, A.; McIntosh, J. M.; Job, D.; Giros, B.; Martres, M.-P. Sustained increase of $\alpha 7$ nicotinic receptors and choline-induced improvement of learning deficit in STOP knock-out mice. *Neuropharmacology* **2007**, *52*, 1691–1700.
- (10) Curzon, P.; Anderson, D. J.; Nikkel, A. L.; Fox, G. B.; Gopalakrishnan, M.; Decker, M. W.; Bitner, R. S. Antisense knockdown of the rat $\alpha 7$ nicotinic acetylcholine receptor produces spatial memory impairment. *Neurosci. Lett.* **2006**, *410*, 15–19.
- (11) Jensen, A. A.; Frolund, B.; Liljefors, T.; Krogsgaard-Larsen, P. Neuronal nicotinic acetylcholine receptors: structural revelations, target identifications, and therapeutic inspirations. *J. Med. Chem.* **2005**, *48*, 4705–4745.
- (12) Olincy, A.; Stevens, K. E. Treating schizophrenia symptoms with an $\alpha 7$ nicotinic agonist, from mice to men. *Biochem. Pharmacol.* **2007**, *74*, 1192–1201.

- (13) Boess, F. G.; De Vry, J.; Erb, C.; Flessner, T.; Hendrix, M.; Luthile, J.; Methfessel, C.; Riedl, B.; Schnizler, K.; van der Staay, F.-J.; van Kampen, M.; Wiese, W. B.; Koenig, G. The novel $\alpha 7$ nicotinic acetylcholine receptor agonist *N*-[(3*R*)-1-azabicyclo[2.2.2]oct-3-yl]-7-[2-(methoxyphenyl)-1-benzofuran-2-carboxamide] improves working and recognition memory in rodents. *J. Pharmacol. Exp. Ther.* **2007**, *321*, 716–725.
- (14) Feuerbach, D.; Nozulak, J.; Lingenhoebl, K.; McAllister, K.; Hoyer, D. JN403, in vitro characterization of a novel nicotinic acetylcholine receptor $\alpha 7$ selective agonist. *Neurosci. Lett.* **2007**, *416*, 61–65.
- (15) Pichat, P.; Bergis, O. E.; Terranova, J.-P.; Urani, A.; Duarte, C.; Santucci, V.; Gueudet, C.; Voltz, C.; Steinberg, R.; Stemmelin, J.; Oury-Donat, F.; Avenet, P.; Griebel, G.; Scatton, B. SSR180711, a novel selective $\alpha 7$ nicotinic receptor partial agonist: (II) efficacy in experimental models predictive of activity against cognitive symptoms of schizophrenia. *Neuropsychopharmacology* **2007**, *32*, 17–34.
- (16) Hajos, M.; Hurst, R. S.; Hoffmann, W. E.; Krause, M.; Wall, T. M.; Higdon, N. R.; Groppi, V. E. The selective $\alpha 7$ nicotinic acetylcholine receptor agonist PNU-282987 [*N*-[(3*R*)-1-Azabicyclo[2.2.2]oct-3-yl]-4-chlorobenzamide hydrochloride] enhances GABAergic synaptic activity in brain slices and restores auditory gating deficits in anesthetized rats. *J. Pharmacol. Exp. Ther.* **2005**, *312*, 1213–1222.
- (17) Tatsumi, R.; Fujio, M.; Satoh, H.; Katayama, J.; Takanashi, S.; Hashimoto, K.; Tanaka, H. Discovery of the $\alpha 7$ nicotinic acetylcholine receptor agonists. (*R*)-3'-(5-chlorothiophen-2-yl)spiro-1-azabicyclo[2.2.2]octane-3,5'-[1',3']oxazolidin-2'-one as a novel, potent, selective, and orally bioavailable ligand. *J. Med. Chem.* **2005**, *48*, 2678–2686.
- (18) Edelstein, S. J.; Changeux, J.-P. Allosteric transitions of the acetylcholine receptor. *Adv. Protein Chem.* **1998**, *51*, 121–184.
- (19) Bertrand, D.; Gopalakrishnan, M. Allosteric modulation of nicotinic acetylcholine receptors. *Biochem. Pharmacol.* **2007**, *74*, 1155–1163.
- (20) Mohler, H.; Fritschy, J. M.; Rudolph, U. A new benzodiazepine pharmacology. *J. Pharmacol. Exp. Ther.* **2002**, *300*, 2–8.
- (21) Kenakin, T. P. Characteristics of Allosterism in Drug Action. In *Allosteric Receptor Modulation in Drug Targeting*; Bowery, N. G., Ed.; Taylor & Francis Group: New York, 2006; pp 19–37.
- (22) Hall, D. A. Predicting Dose–Response Curve Behavior. In *Allosteric Receptor Modulation in Drug Targeting*; Bowery, N. G., Ed.; Taylor & Francis Group: New York, 2006; pp 39–78.
- (23) Faghih, R.; Gopalakrishnan, M.; Briggs, C. A. Allosteric modulator of the $\alpha 7$ nicotinic acetylcholine receptor. *J. Med. Chem.* **2008**, *51*, 701–712.
- (24) Changeux, J.-P. The TiPS Lecture—The Nicotinic Acetylcholine Receptor—An Allosteric Protein Prototype of Ligand-Gated Ion Channels. *Trends Pharmacol. Sci.* **1990**, *11*, 485–492.
- (25) Butt, C. M.; Hutton, S. R.; Marks, M. J.; Collins, A. C. Bovine serum albumin enhances nicotinic acetylcholine receptor function in mouse thalamic synaptosomes. *J. Neurochem.* **2002**, *83*, 48–56.
- (26) Adermann, K.; Wattler, F.; Wattler, S.; Heine, G.; Meyer, M.; Forssmann, W. G.; Nehls, M. Structural and phylogenetic characterization of human SLURP-1, the first secreted mammalian member of the Ly-6/uPAR protein superfamily. *Protein Sci.* **1999**, *8*, 810–819.
- (27) Charpentier, E.; Wiesner, A.; Huh, K. H.; Ogier, R.; Hoda, J. C.; Allaman, G.; Raggenbass, M.; Feuerbach, D.; Bertrand, D.; Fuhrer, C. $\alpha 7$ neuronal nicotinic acetylcholine receptors are negatively regulated by tyrosine phosphorylation and Src-family kinases. *J. Neurosci.* **2005**, *25*, 9836–9849.
- (28) Samochocki, M.; HOFFLE, A.; Fehrenbacher, A.; Jostock, R.; Ludwig, J.; Christner, C.; Radina, M.; Zerlin, M.; Ullmer, C.; Pereira, E. F. R.; Lubbert, H.; Albuquerque, E. X.; Maelicke, A. Galantamine is an allosterically potentiating ligand of neuronal nicotinic but not of muscarinic acetylcholine receptors. *J. Pharmacol. Exp. Ther.* **2003**, *305*, 1024–1036.
- (29) Zwart, R.; De Filippi, G.; Broad, L. M.; McPhie, G. I.; Pearson, K. H.; Baldwin, T.; Sher, E. 5-Hydroxyindole potentiates human $\alpha 7$ nicotinic receptor-mediated responses and enhances acetylcholine-induced glutamate release in cerebellar slices. *Neuropharmacology* **2002**, *43*, 374–384.
- (30) Ng, H. J.; Whittemore, E. R.; Tran, M. B.; Hogenkamp, D. J.; Broide, R. S.; Johnstone, T. B.; Zheng, L.; Stevens, K. E.; Gee, K. W. Nootropic $\alpha 7$ nicotinic receptor allosteric modulator derived from GABA_A receptor modulators. *Proc. Natl. Acad. Sci. U.S.A.* **2007**, *104*, 8059–8064.
- (31) Timmermann, D. B.; Grønlien, J. H.; Kohlhaas, K. L.; Nielsen, E. Ø.; Dam, E.; Jørgensen, T. D.; Ahring, P. K.; Peters, D.; Holst, D.; Christensen, J. K.; Malysz, J.; Briggs, C. A.; Gopalakrishnan, M.; Olsen, G. M. An allosteric modulator of the $\alpha 7$ nicotinic acetylcholine receptor displaying memory enhancing properties. *J. Pharmacol. Exp. Ther.* **2007**, *323*, 294–307.
- (32) Hurst, R. S.; Hajos, M.; Raggenbass, M.; Wall, T. M.; Higdon, N. R.; Lawson, J. A.; Rutherford-Root, K. L.; Berkenpas, M. B.; Hoffmann, W. E.; Piotrowski, D. W.; Groppi, V. E.; Allaman, G.; Ogier, R.; Bertrand, S.; Bertrand, D.; Arneric, S. P. A novel positive allosteric modulator of the $\alpha 7$ neuronal nicotinic acetylcholine receptor: in vitro and in vivo characterization. *J. Neurosci.* **2005**, *25*, 4396–4405.
- (33) Grønlien, J. H.; Haakerud, M.; Ween, H.; Thorin-Hagene, K.; Briggs, C. A.; Gopalakrishnan, M.; Malysz, J. Distinct profiles of $\alpha 7$ nAChR positive allosteric modulation revealed by structurally diverse chemotypes. *Mol. Pharmacol.* **2007**, *72*, 715–724.
- (34) Broad, L. M.; Zwart, R.; Pearson, K. H.; Lee, M.; Wallace, L.; McPhie, G. I.; Emkey, R.; Hollinshead, S. P.; Dell, C. P.; Baker, S. R.; Sher, E. Identification and pharmacological profile of a new class of selective nicotinic acetylcholine receptor potentiators. *J. Pharmacol. Exp. Ther.* **2006**, *318*, 1108–1117.
- (35) Dinklo, T.; Meeus, K.; Peeters, L.; Lavreysen, H.; van Roosbroeck, Y.; Grantham, C. J.; Vandenberk, I.; Pouzet, B.; Stevens, K. E.; Zheng, L.; Mackie, C.; Macdonald, G.; Lesage, A.; Thuring, J. In vitro and in vivo evaluation of JNJ1930942, a novel $\alpha 7$ nAChR selective positive allosteric modulator. *Biochem. Pharmacol.* **2007**, *74*, SMA-33.
- (36) Ferreira, V. F.; De Souza, M. C. B. V.; Cunha, A. C.; Pereira, L. O. R.; Ferreira, M. L. G. Recent advances in the synthesis of pyrroles. *Org. Prep. Proc. Int.* **2001**, *33*, 411–454.
- (37) Singh, J.; Satyamurthi, N.; Aidhen, I. S. The growing synthetic utility of Weinreb's amide. *J. Prakt. Chem.* **2000**, *342*, 340–347.
- (38) Keck, G. E.; Sanchez, C.; Wager, C. A. Macrolactonization of hydroxy acids using a polymer-bound carbodiimide. *Tetrahedron Lett.* **2000**, *41*, 8673–8676.
- (39) Briggs, C. A.; McKenna, D. G. Activation and inhibition of the human $\alpha 7$ nicotinic acetylcholine receptor by agonists. *Neuropharmacology* **1998**, *37*, 1095–1102.
- (40) Malysz, J.; Grønlien, J. H.; Anderson, D. J.; Haakerud, M.; Thorin-Hagene, K.; Ween, H.; Briggs, C. A.; Faghih, R.; Bunnelle, W. H.; Gopalakrishnan, M. In vitro pharmacological profile of A-867744: a novel type II $\alpha 7$ nAChR PAM exhibiting a unique pharmacological profile. *Soc. Neurosci. Abstr.* **2008**, 233.10/C12.
- (41) Gopalakrishnan, S. M.; Philip, B. M.; Anderson, D. J.; Malysz, J.; Burns, D. J.; Gopalakrishnan, M.; Warrior, U. Functional characterization of positive allosteric modulators of $\alpha 7$ nicotinic acetylcholine receptors in IMR-32 neuroblastoma cells. *Soc. Biomol. Screening Abstr.* **2008**, P15006.
- (42) Leonard, S.; Bresse, C.; Adams, C.; Benhammou, K.; Gault, J.; Stevens, K.; Lee, M.; Adler, L.; Olincy, A.; Ross, R.; Freedman, R. Smoking and schizophrenia: abnormal nicotinic receptor expression. *Eur. J. Pharmacol.* **2000**, *393*, 237–242.
- (43) Stevens, K. E.; Kem, W. R.; Mahnir, V. M.; Freedman, R. Selective $\alpha 7$ -nicotinic agonists normalize inhibition of auditory response in DBA mice. *Psychopharmacology* **1998**, *136*, 320–327.
- (44) Radek, R. J.; Miner, H. M.; Bratcher, N. A.; Decker, M. W.; Gopalakrishnan, M.; Bitner, R. S. $\alpha 4\beta 2$ Nicotinic receptor stimulation contributes to the effects of nicotine in the DBA/2 mouse model of sensory gating. *Psychopharmacology* **2006**, *187*, 47–55.